Supporting information: Printing of Tin Perovskite Solar Cells via Controlled Crystallization

Xuan Li[a,e,#], Giuseppe Nasti[b,c,#], Chris Dreessen[d], Janardan Dagar[e], Rico Meitzner[e], Davide Amoroso[c], Pier Luca Maffettone[c], Thomas Kirchartz[d,f], Eva Unger[e], Antonio Abate[c,e,*], Stoichko D. Dimitrov[a,*]

Authors and Affiliations

a) Department of Chemistry, School of Physical and Chemical Sciences, Queen Mary University of London, E1 4NS London, U.K

b) ENEA Research Center Portici, Piazzale Enrico Fermi 1, Portici, 80055 Italy

c) Department of Chemical, Materials and Production Engineering, University of Naples Federico II, Piazzale Tecchio 80, Naples, Fuorigrotta, 80125 Italy

d) IEK5-Photovoltaik, Forschungszentrum Jülich, 52425 Jülich, Germany

e) Helmholtz-Zentrum Berlin für Materialien und Energie GmbH, Hahn-Meitner-Platz 1, 14109 Berlin, Germany

f) Faculty of Engineering and CENIDE, University of Duisburg-Essen, Carl-Benz-Str. 199, 47057 Duisburg, Germany

Table S 1: Parameters of each film during the gas pulse trigger and after annealing estimated from PL.

Additives Used for $FASnI_3$ Films	Band gap (eV) Gas Pulse Trigger	Band gap (eV) Prior annealing	Band gap (eV) Annealed	Δ E (eV) Gas Pulse Trigger to before annealing	Δ E (eV) Gas Pulse Trigger to Annealed	Δ E (eV) Gas Pulse Trigger to Annealed	Intensity Annealed	FWHM (eV)
$SnCl_2$	1.82	1.57	1.41	-0.25	-0.16	-0.41	7259	0.087
MACl	-	-	1.52	-	-	-	3434	0.105
$MASnCl_3$	1.73	1.51	1.42	-0.22	-0.09	-0.31	17205	0.095
SnF_2	1.81	1.51	1.42	-0.30	-0.09	-0.39	9003	0.090

Table S 2: XRD peaks and corresponding species.

Additive/Species	NA	SnI_4	$FASnI_3$ (100)	SnI_4	NA	$FASnI_3$ (200)	$FASnI_3$ (122)
$SnCl_2$		12.75 12.94	14.30	25.73	26.24	29.18	
MACl		12.87	14.04	25.53	26.13	28.71	31.55
$MASnCl_3$			14.31			29.08	
SnF_2	12.24		14.17			28.91	

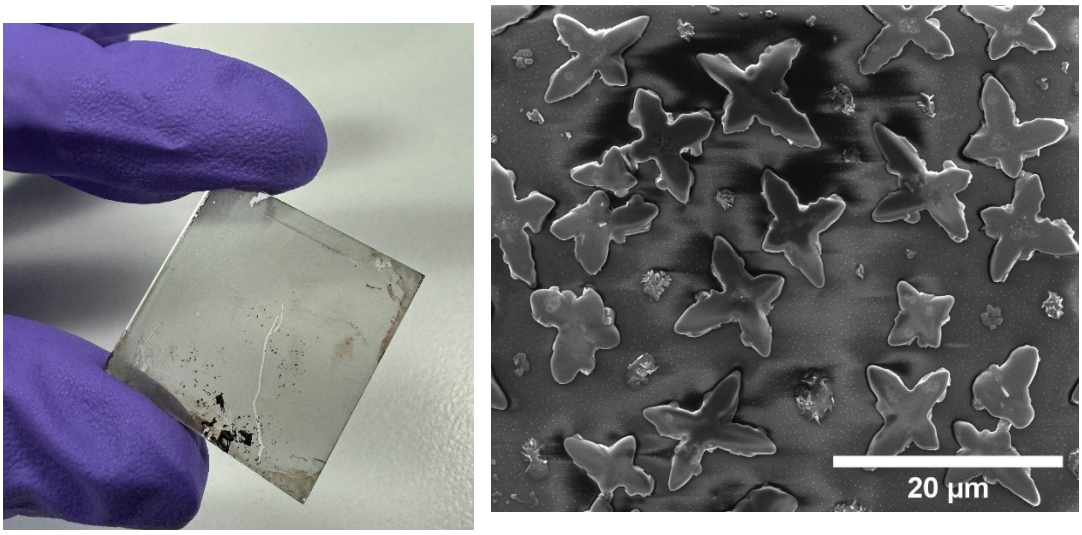

Figure S 1: Photo and SEM image of $FASnI_3$ films produced without the gas pulse step.

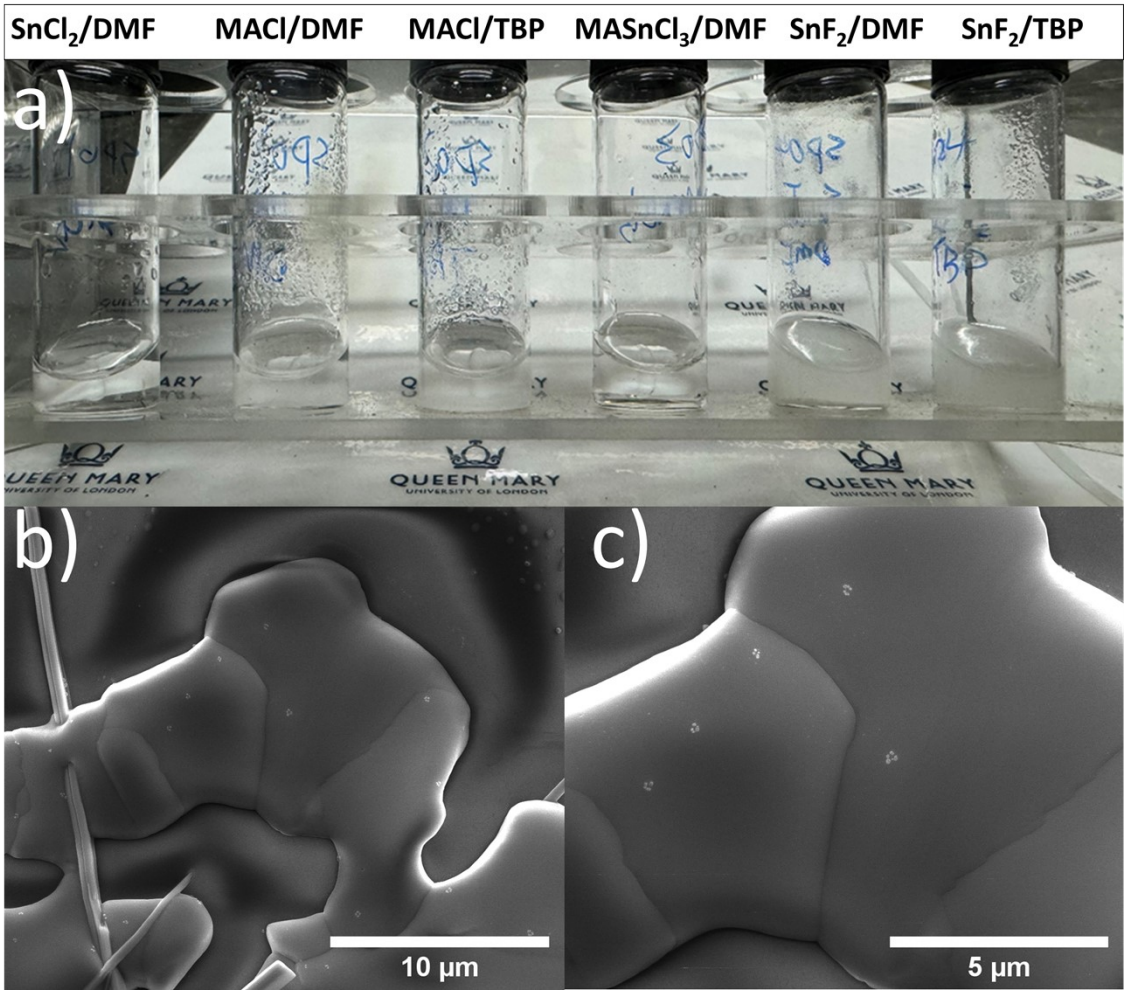

Figure S 2: a): Solubility test of additives in DMF (1 M concentration tested); b) and c): SEM images of spin coated 1 M $MASnCl_3$ in DMF from gas pulse quenching similar to the spin coating process for the $FASnI_3$ film. Massive grains were observed under SEM. This indicates the possibility to prepare pure $MASnCl_3$ films.

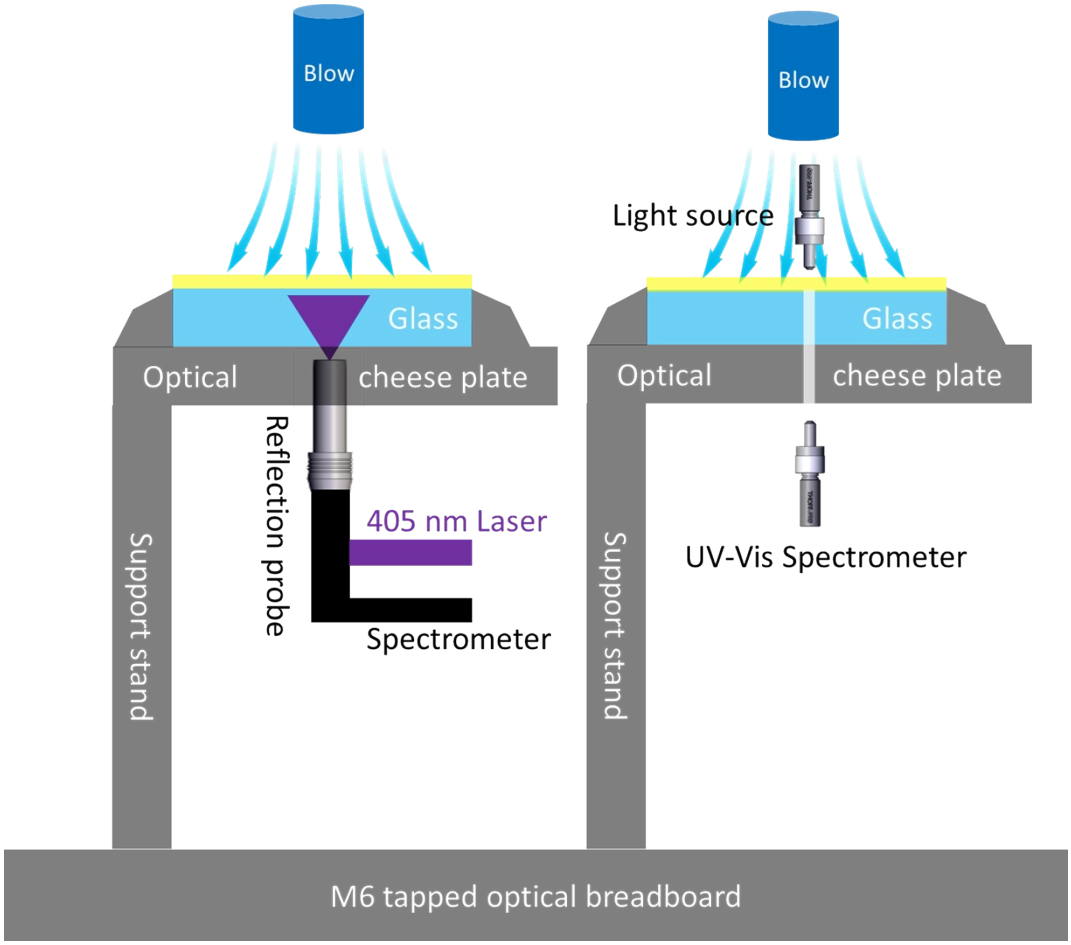

Figure S 3: Set-up of the in-situ measurement. Wet film was placed immediately on to the cheese plate after printing and in-situ monitoring started right before gas pulse applied.

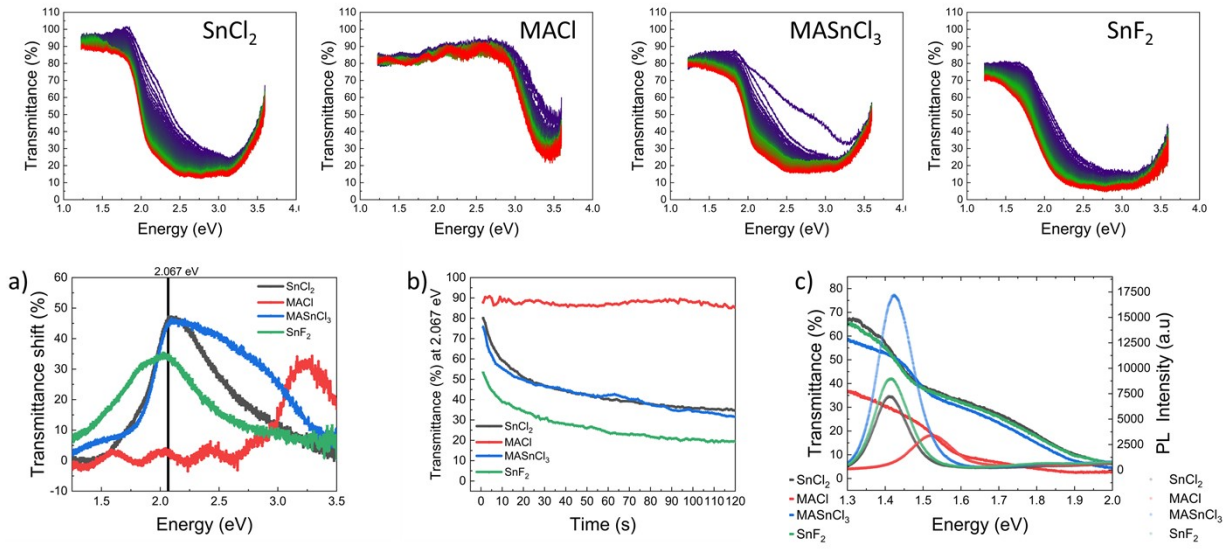

Figure S 4: Top row: In-situ transmittance data during 120 s after gas pulsing (blue being the 1st measurement and red being the final 120th measurement). a): Transmittance shift (the mathematical difference between the 1st transmittance data after the gas pulse and the 120th final transmittance data after gas pulse), indicating the energy location where the biggest change happened. b): Transmittance shift tracking at 2.067 eV. c): Steady-state final PL and final transmittance after thermal annealing.

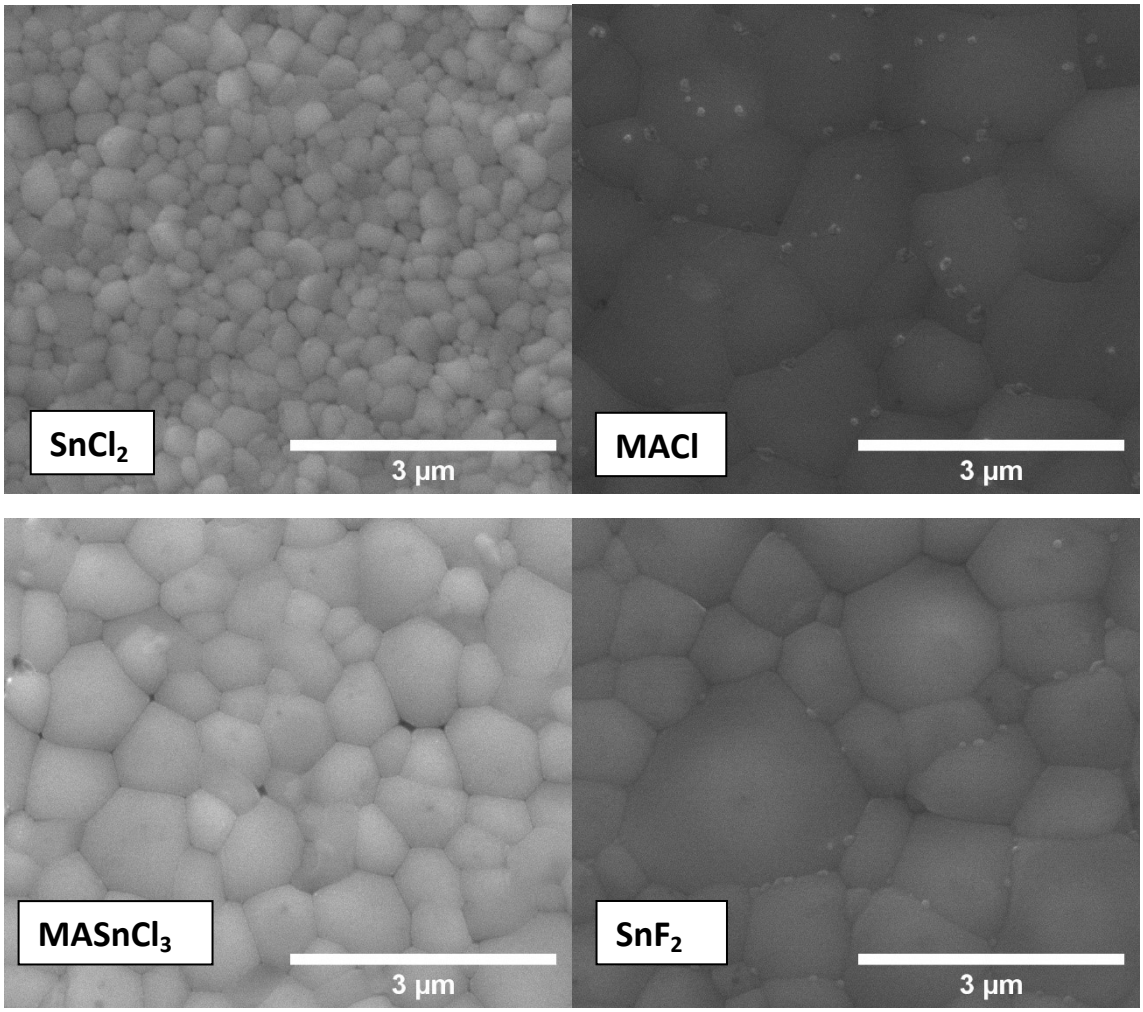

Figure S 5: SEM images of slod die coated FASI-$SnCl_2$, FASI-MACl, FASI-$MASnCl_3$ and FASI-SnF_2 films on glass substrates produced using gas pulse trigger and heating.

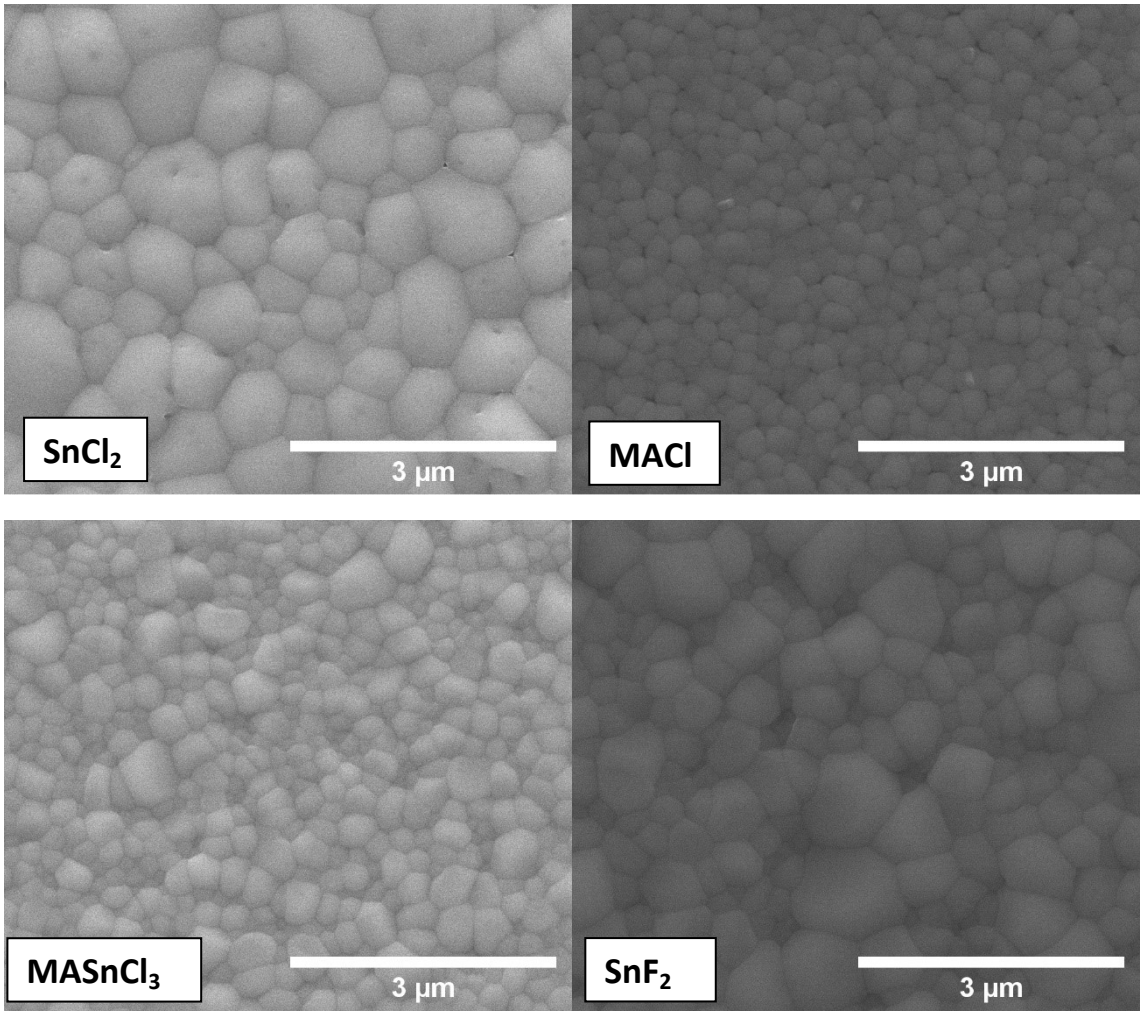

Figure S 6: SEM images of slod die coated FASI-$SnCl_2$, FASI-MACl, FASI-$MASnCl_3$ and FASI-SnF_2 films on PEDOT:PSS/ITO glass substrates produced using a gas pulse trigger and heating.

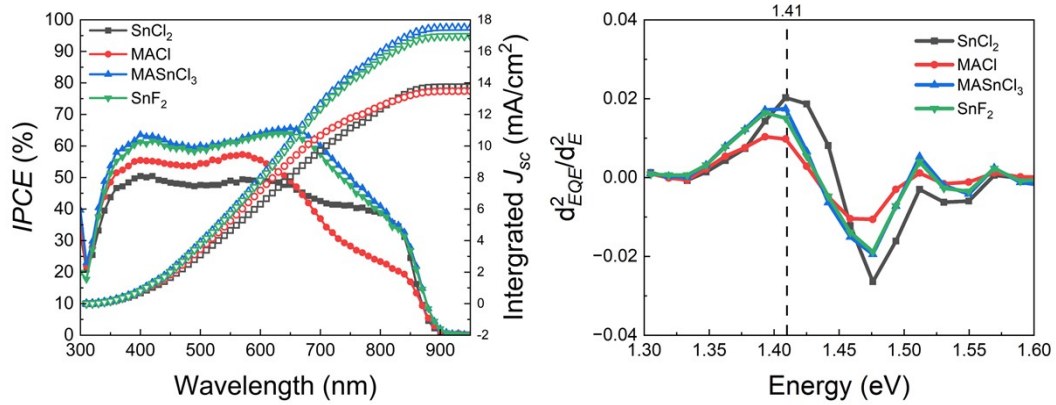

Figure S 7: IPCE measurement of the champion pixels of each FASI-Additive device, and the corresponding $(d_{EQE})^2/(d_E)^2$ plot identifying the band gap value. The IPCE values integrate to a higher JSC than the estimates from our JV measurements.
Figure S7: The IPCE values integrate to a higher JSC than the estimates from our JV measurements. The results from the JV

scans of the record pixels are reported as they were recorded right after fabrication. The IPCE and JV measurements show the same trend in photocurrent changes with additive.

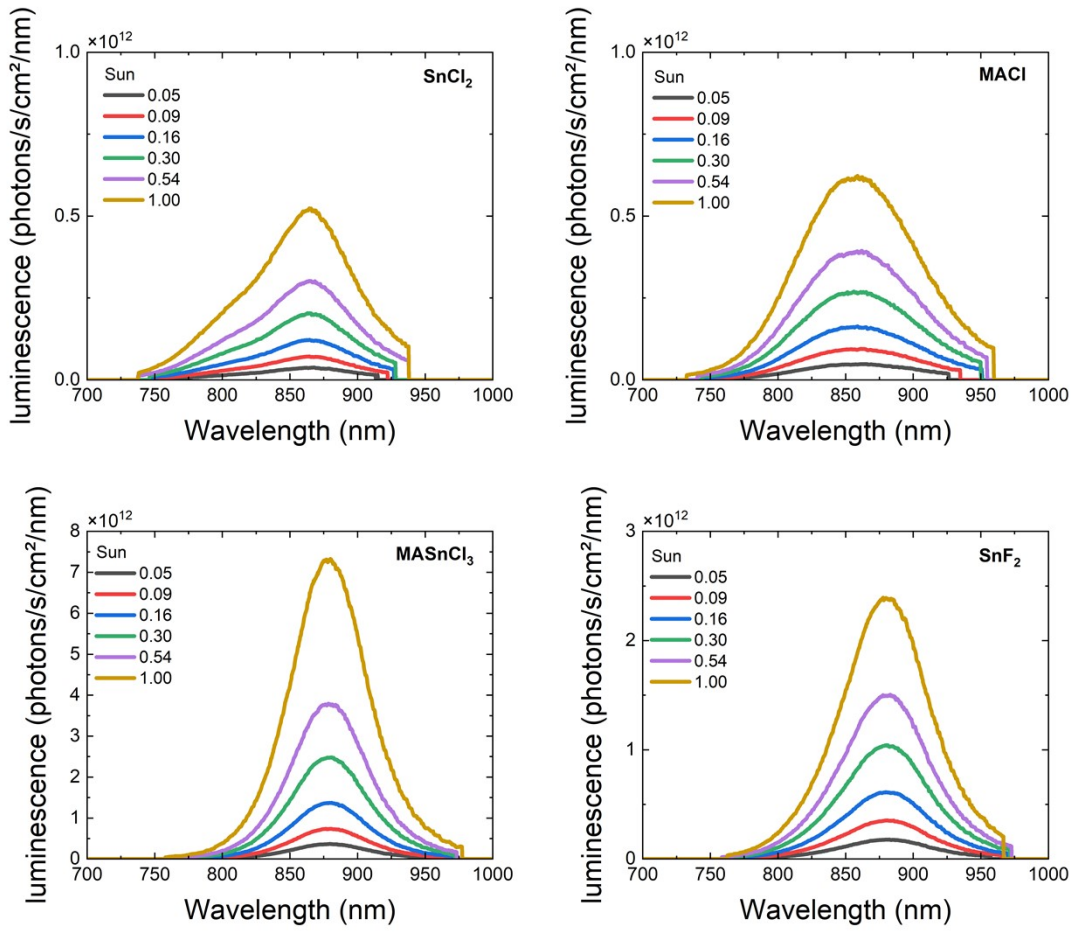

Figure S 8: Light-dependent photoluminescence spectra of each device with different additives. Note the scale bar differences that FASI-MASnCl$_3$ device has the highest PL intensity.

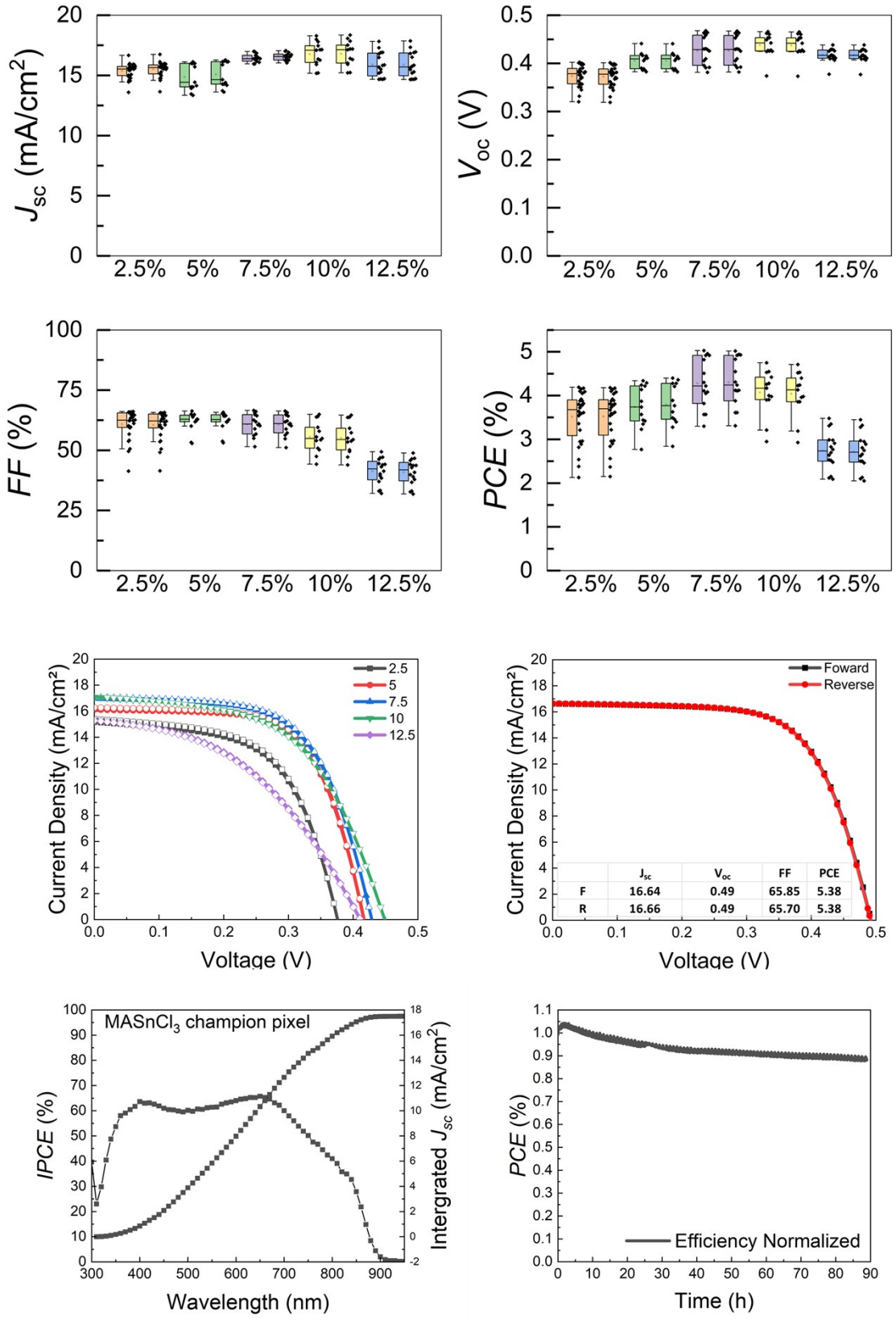

Figure S 9: Performance (forward and reverse scans) distribution of $MASnCl_3$ molar concentration. The champion pixel is from 7.5 M%.

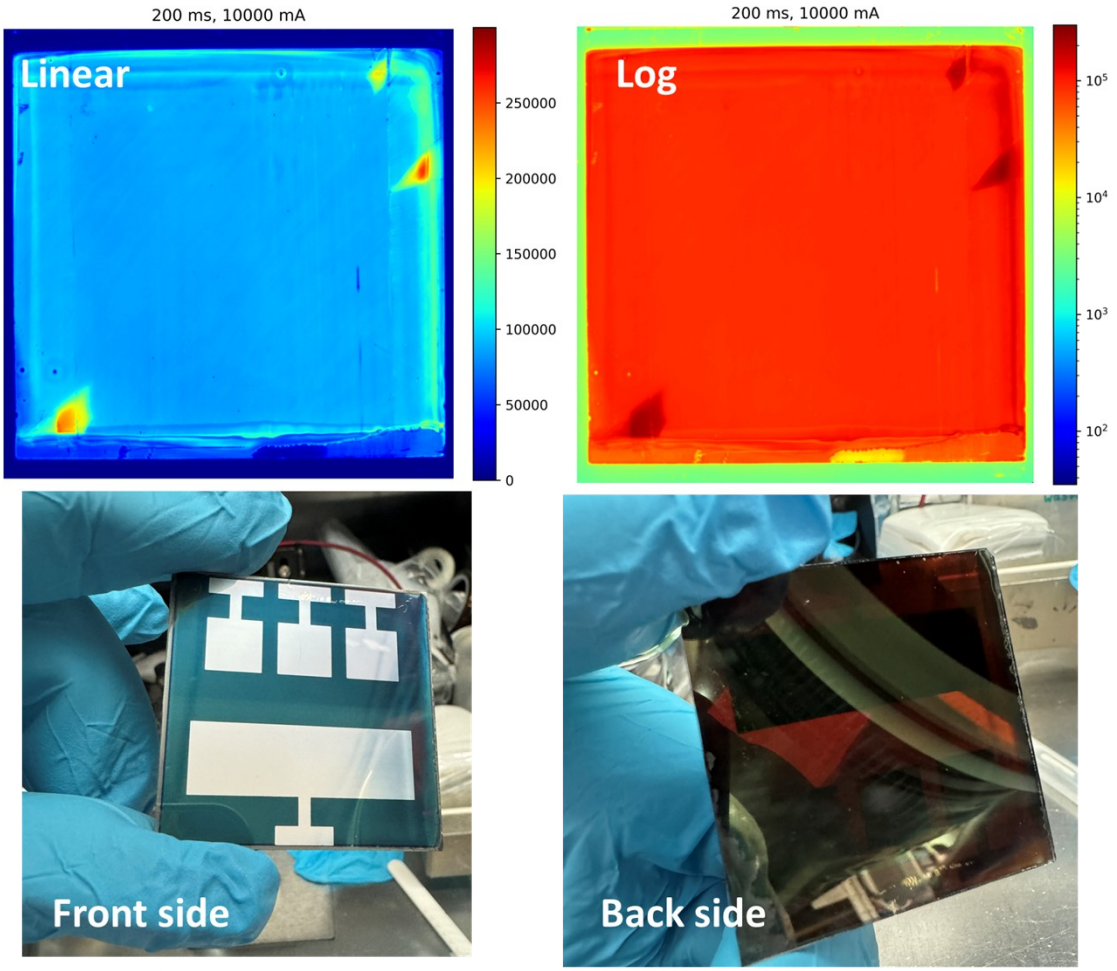

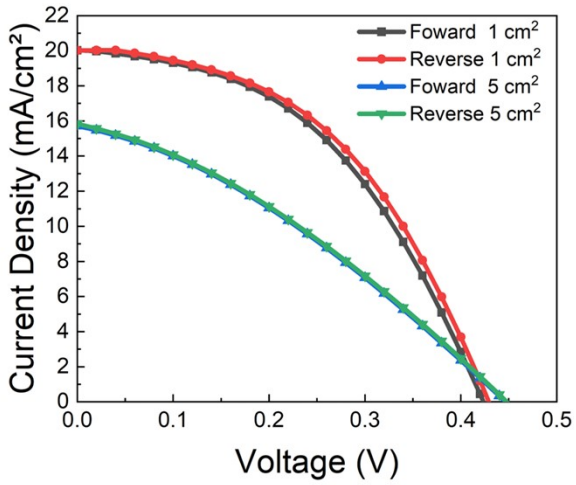

Area	J_{sc} (mA/cm^2)	V_{oc} (V)	*FF*	*PCE* (%)
1 cm^2 F	20.02	0.42	45.7	3.88
1 cm^2 R	20.01	0.43	46.9	4.02
5 cm^2 F	15.71	0.45	32.7	2.29
5 cm^2 R	15.83	0.44	32.68	2.31

Figure S 10: Photoluminescence Imaging of the deposited $FASnI_3$ films on ITO/PEDOT:PSS, the bright spots in the absolute plot corresponds to uncovered PEDOT layer from spin coating process. The photos of the front and back side of the 50x50mm device. The JV scan results of the champion performances of the 1 cm^2 and 5 cm^2 pixels.

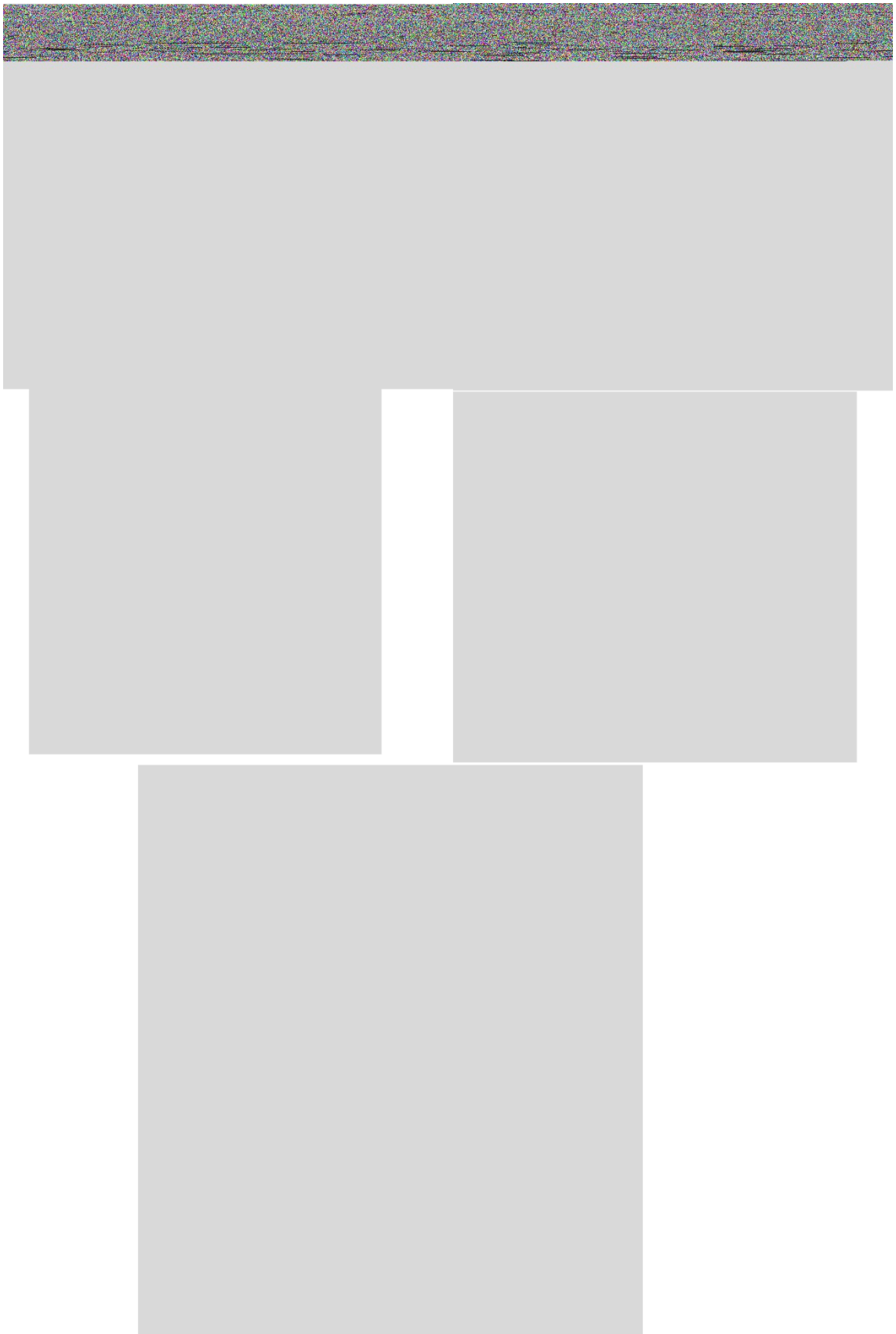

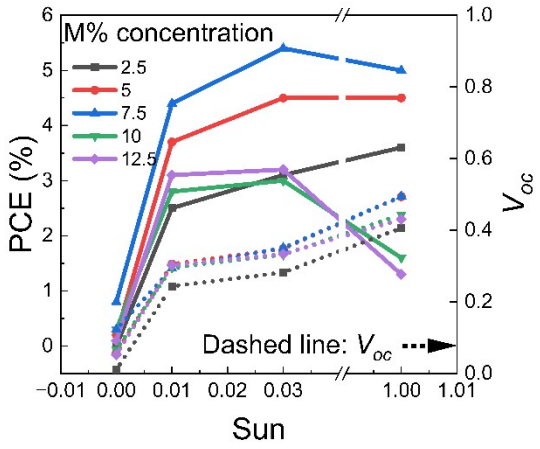

Figure S 11: Device response to low light level LED illumination, including V_{OC} changes (broken lines connect V_{OC} data points) as a function of light intensity. PCE data corresponds to data in Figure 4 in the main text.